DEPARTMENT OF PHYSICS AND GEOPHYSICAL SCIENCES
SCHOOL OF SCIENCES AND HEALTH PROFESSIONS
OLD DOMINION UNIVERSITY
NORFOLK, VIRGINIA

Technical Report PGSTR-PH77-51

A STUDY ON CHARACTERIZATION OF STRATOSPHERIC AEROSOL AND GAS PARAMETERS WITH THE SPACECRAFT SOLAR OCCULTATION EXPERIMENT

By

William P. Chu

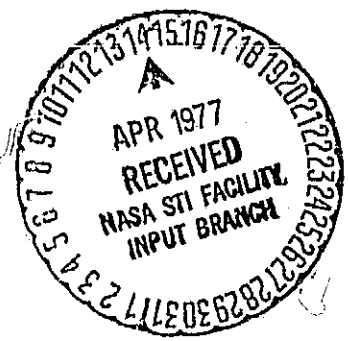

Final Report

Prepared for the
National Aeronautics and Space Administration
Langley Research Center
Hampton, Virginia

Under
NASA Grant NSG 1259
October 1, 1975 - December 31, 1976
M. P. McCormick, Technical Monitor
Instrument Research Division

March 1977

OLD DOMINION UNIVERSITY RESEARCH FOUNDATION

DEPARTMENT OF PHYSICS AND GEOPHYSICAL SCIENCES
SCHOOL OF SCIENCES AND HEALTH PROFESSIONS
OLD DOMINION UNIVERSITY
NORFOLK, VIRGINIA

Technical Report PGSTR-PH77-51

A STUDY ON CHARACTERIZATION OF STRATOSPHERIC AEROSOL AND GAS PARAMETERS WITH THE SPACECRAFT SOLAR OCCULTATION EXPERIMENT

By

William P. Chu

Final Report

Prepared for the
National Aeronautics and Space Administration
Langley Research Center
Hampton, Virginia 23665

Under
NASA Grant NSG 1259
October 1, 1975 - December 31, 1976
M. P. McCormick, Technical Monitor
Instrument Research Division

Submitted by
Old Dominion University Research Foundation
Norfolk, Virginia 23508

March 1977

A STUDY ON CHARACTERIZATION OF STRATOSPHERIC AEROSOL AND GAS PARAMETERS WITH THE SPACECRAFT SOLAR OCCULTATION EXPERIMENT

By

William P. Chu[1]

SUMMARY

This report contains results of research investigations performed during the period from October 1975 to December 1976 under NASA Grant NSG 1259. Spacecraft remote sensing of stratospheric aerosol and ozone vertical profiles using the solar occultation experiment has been analyzed. A computer algorithm has been developed in which a two-step inversion of the simulated data can be performed. The radiometric data are first inverted into a vertical extinction profile using a linear inversion algorithm. Then the multiwavelength extinction profiles are solved with a nonlinear least-square algorithm to produce aerosol and ozone vertical profiles. Examples of inversion results are shown illustrating the resolution and noise sensitivity of the inversion algorithms.

INTRODUCTION

The minor constituents in the stratosphere have received great attention in recent years because of concerns over their roles in affecting the global environment. With mankind's increasing activities in the stratosphere such as SST and Shuttle missions, and ground-based activities such as those involved with nitrogen fertilizers, an increase in stratospheric aerosol loading together with the removal of stratospheric ozone are possible through various chemical reactions. A realistic assessment of this problem is still not possible due to the lack of information on the distributions of most of the constituents in our atmosphere.

---

[1] Research Associate, Old Dominion University, Norfolk, Virginia 23508.

This report analyzes one of the atmospheric remote sensing methods using spacecraft solar extinction technique to retrieve stratospheric aerosol and ozone vertical profiles. In this remote sensing technique, the spacecraft instrument will direct towards the horizon and measure transmitted solar radiant intensity in a number of spectral intervals from 0.38 to 1.00 micron wavelength. The locations of the spectral channels are selected based on considerations of maximum extinction contributed from any individual constituent, interference from other constituents, and available energy for measurements. The radiant intensity data are then inverted to produce vertical profiles for each of the constituents. The inversion procedure can be separated into two steps. The first step involved retrieval of the total vertical extinction profiles at each spectral interval. The second step then separated the contributions from each constituent using the multispectral extinction data at each altitude level. Examples of inverted results from simulated data including experimental errors are presented and discussed in this paper.

EXPERIMENTAL CONCEPT

In the solar extinction experiment, multiwavelength measurements of the transmitted solar radiant intensity along the line of sight through the atmosphere are made on board the spacecraft. The basic geometry is illustrated in figure 1. As the spacecraft emerges from Earth's shadow, the radiometer aboard the spacecraft will point to the sun, measuring solar radiant intensity at several preselected wavelength regions. In this paper we will consider a radiometer with a small field of view in order to achieve higher vertical resolution. The radiometer is assumed to either lock on a fixed position on the solar disk or scan across the solar disk for data acquisition.

The monochromatic radiant intensity reaching the radiometer is given by the fundamental equation of radiative transfer (Chandrasekhar, 1950).

$$I_\lambda(h_z) = I_\lambda(h_o)\ \tau_\lambda(h_z,h_o) + \int_{\tau_\lambda(h_z,h_o)}^{1} J_\lambda(h)\ d\tau_\lambda(h_z,h) \qquad (1)$$

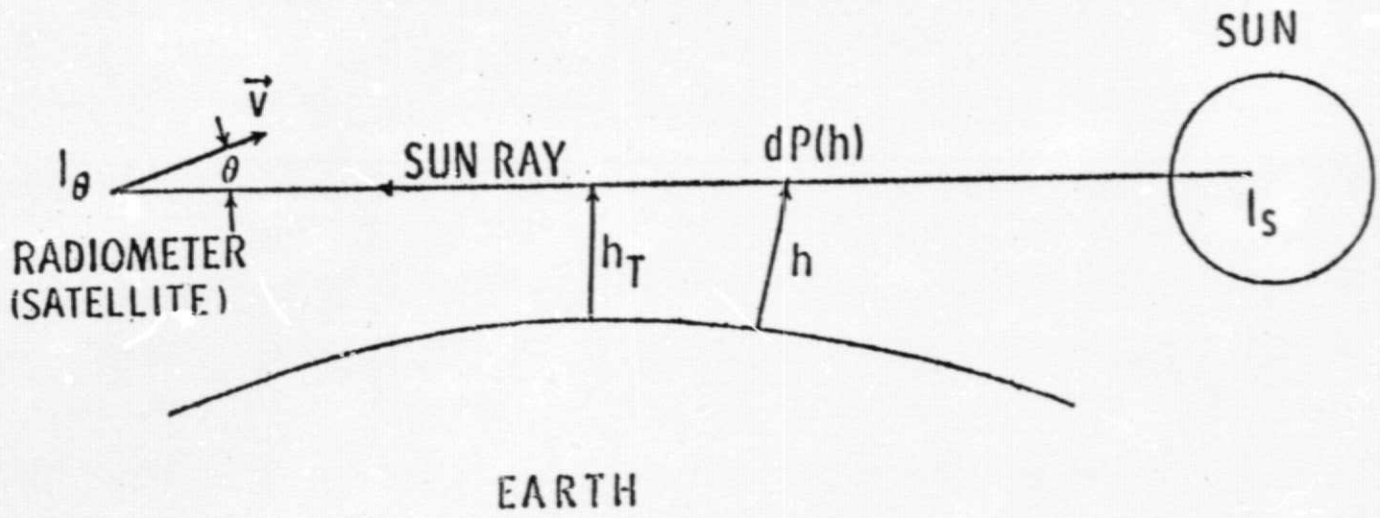

SOLAR OCCUTATION GEOMETRY

$$I_\theta = \tau[h_T(\theta)]\, I_S$$

LAMBERT-BEER LAW

$$\tau(h_T) = \mathrm{EXP}\left\{-2\int_{h_T}^{\infty} \beta(h)\, dP(h)\right\}$$

$\beta(h)$ - EXTINCTION PROFILE

$P(h)$ - REFRACTED OPTICAL PATH

Figure 1. Geometry of the solar extinction experiment.

The above equation relates at wavelength λ, the radiant intensity $I_\lambda(h_z)$ measured at distance h_z, to the radiant intensity $I_\lambda(h_o)$ at boundary h_o, the monochromatic transmittance $\tau_\lambda(h_z,h_o)$ and source function $J_\lambda(h)$ at distance h along path from h_z to h_o.

For the solar extinction experiment with spectral channels closed to the visible region, the contribution by atmospheric emission to the radiant intensity is very small and can safely be neglected. The radiative transfer equation is thus greatly simplified to

$$I_\lambda(h_z) = I_\lambda(h_o)\ \tau_\lambda(h_z,h_o) \tag{2}$$

where the radiant intensity $I_\lambda(h_o)$ is now the solar radiant intensity, and $\tau_\lambda(h_z,h_o)$ is the transmittance of the atmosphere between the sun and the spacecraft.

In the wavelength range from 0.3 to 1.0 micron, atmospheric attenuation are predominantly caused by aerosol, ozone, and air molecules (Rayleigh component) with minor contributions from NO_2, water vapor and O_2 molecules. The model of the stratospheric extinction versus wavelength profile can be constructed from different vertical distributions of aerosol and ozone. Figure 2 shows an extinction coefficient model as a function of wavelength at an altitude of 18 km. Notice that at most of the wavelength shown, the total extinction consists of contributions from aerosol, ozone, and Rayleigh component with different weights. The weightings will also be different for different altitude levels, depending on the distributions of the different constitutents.

If we made the assumptions that the atmosphere is spherically stratified and spherically symmetric, the transmittance function $\tau_\lambda(h_z,h_o)$ will then be given by the Lambert-Beer law as

$$\tau_\lambda(h_z,h_o) = \exp\ \{-\ 2 \int_{h_T}^{\infty} \beta_\lambda(h)\ dP(h,h_T)\} \tag{3}$$

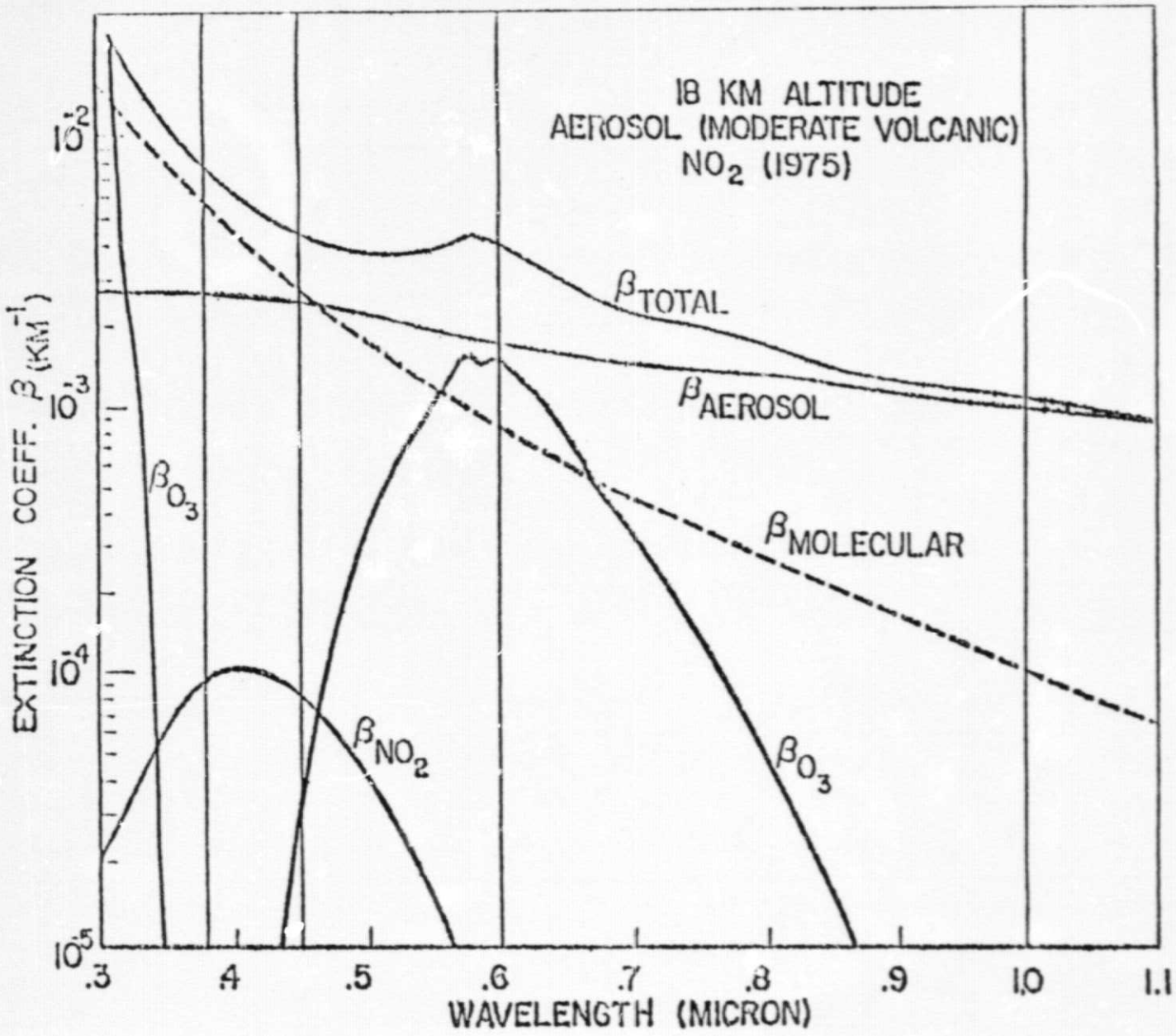

Figure 2. Atmospheric extinction versus wavelength model at an altitude of 18 km.

where $\beta_\lambda(h)$ is the atmospheric extinction coefficient at wavelength λ versus vertical height h, $P(h,h_T)$ is the optical path at height h for line of sight with tangent height h_T. Equivalently, we can define the optical depth $g_\lambda(h_T)$ as

$$g_\lambda(h_T) = \ln \{1/\tau_\nu(h_z,h_o)\}$$

$$= 2 \int_{h_T}^{\infty} \beta_\lambda(h)\, dP(h,h_T) \qquad (4)$$

The determination of vertical extinction profile at each wavelength λ required the inversion of the integral in equation (4).

INVERSION TECHNIQUES

Inversion of Measured Transmittance to Total Extinction Profiles

In equation (4), the measured parameter $g_\lambda(h_T)$ is equal to a kind of convolution of the weighting function $\partial P(h,h_T)/\partial h$ with the unknown vertical extinction profile $\beta_\lambda(h)$. The integral can be approximated with a sum over n discrete atmospheric layers with equal thickness and assigning to each layer an averaged extinction coefficient β_j. The integral equation can then be replaced by a system of linear equations.

$$g_i = \sum_{j=i}^{n} \beta_j P_{ij} \qquad i = 1, 2, \ldots m \qquad (5)$$

where P_{ij} is the optical path length in the jth layer with tangent height at the ith layer. Equation (5) can be abbreviated into matrix form

$$g = P\beta \qquad (6)$$

where g is the column vector for the measured optical depth, β is the column vector for the unknown extinction profile, and P is the optical path length matrix.

Equation (6) can be solved directly for β either exactly when $n = m$ or in the least square sense when $n < m$

$$\beta = P^{-1} g \qquad n = m \tag{7a}$$

$$\beta = (P^T P)^{-1} P^T g \qquad n < m \tag{7b}$$

where P^{-1} is the inverse of P and P^T is the transpose of P. The solutions obtained from the direct inversion are generally unstable due to the presence of noise associated with the measured parameter g. In order to suppress the unphysical oscillations in the inverted solutions, some constraints on the high frequency components of the solutions have to be incorporated in the inversion schemes. We have analyzed two different inversion methods. The first method is the linear constrained inversion as developed by Twomey (1963) and Philips (1962); the second method is the iterative scheme recently developed by Twomey (1975). We will discuss the two methods separately below.

Linear constraint inversion

The solution to equation (6) is given by the following expression

$$\beta = (P^T P + \gamma H)^{-1} P^T g \tag{8}$$

where normally H is the constrained matrix, and γ is a constant smoothing parameter. In our analysis, we used the constrained matrix H which minimizes the second difference of the solution. The smoothing parameter γ whose magnitude is proportional to the noise level of the measurements has been replaced by a diagonal matrix of element γ_{ii}. The reason for using a variable smoothing parameter γ arises from the nonlinear expression for the noise term in equation (4). Assuming the radiometer has a noise level e_i associated with each radiant measurement I_i. The deduced transmittance τ_i

will have approximately the same noise level e_i . By computing the optical depth g_i , we have

$$g_i = \ln \{1/(\tau_i + e_i)\} \tag{9}$$

For $e_i << \tau_i$, we can expand (9) and obtain

$$g_i \sim \ln \{1/\tau_i\} - e_i/\tau_i \tag{10}$$

The second term on the right side of the equivalent noise level for the parameter g_i . Thus we choose the matrix element γ_{ii} as

$$\gamma_{ii} = \gamma_o \left(\frac{e_i}{\tau_i}\right) / g_i \tag{11}$$

where γ_o is a constant parameter to be adjusted for optimum inverted solutions.

Iterative inversion

The iterative method starts by initially assumed a guessed solution, then the solution is continuously updated through the following iteration,

$$\beta_j^{(k+1)} = \beta_j^{(k)} + (\gamma_i^{(k)} - 1)\ K_{ij}\ \beta_j^{(k)} \tag{12}$$

where $\beta_j^{(k)}$ is the solution β_j at k-iteration, $\gamma_i^{(k)}$ is the ratio of measured g_i to the computed g_i from the k-iterated solution, and K_{ij} is the normalized weighting function $\partial P(h,h_T)/\partial h$ where $K_{ij} \leq 1$. The iterative process is terminated when the computed radiant approaches the measured radiant to within the instrument noise level.

Inversion of Multiwavelength Extinction Profiles into Constituent Profiles

The inversion methods discussed in the previous section will generate multispectral extinction vertical profiles from the multichannel extinction

measurements. The second step in the inversion process will be to separate the contributions from individual constituents. For the wavelength region of interest, the total extinction coefficient at a fixed altitude level can be written as the sum of contributions from aerosol, ozone, and air molecules as

$$\beta_{total} = \beta_{aerosol}(\lambda) + a_{\lambda i}\, \beta_{mol}(\lambda_o) + b_{\lambda i}\, \beta_{\theta_3}(\lambda_o) \tag{13}$$

where $\beta_{mol}(\lambda_o)$ is the Rayleigh extinction coefficient at a reference wavelength λ_o, $a_{\lambda i}$ is the wavelength dependence of the Rayleigh extinction, $b_{\lambda i}$ is the wavelength dependence of the ozone adsorption profile, and $\beta_{aerosol}(\lambda)$ is the aerosol extinction as a function of wavelength λ. The Rayleigh extinction versus wavelength profile is given by the fourth power law $a_{\lambda i} = (\lambda_o/\lambda_i)^4$. The ozone absorption profile for the Chappuis band has been measured (Inn and Tanaka, 1953). The aerosol extinction versus wavelength dependence is not known and is dependent on aerosol parameters such as shape, size distribution, and complex index refraction. If we assumed the aerosols are all homogeneous spheres, then for a given size distribution $N(r)$, the aerosol extinction profile is given by

$$\beta_{aerosol}(\lambda) = \int_0^\infty \sigma(\lambda,r)\, N(r)\, dr \tag{14}$$

where $\sigma(\lambda,r)$ is the scattering cross section for the spherical aerosol of radius r at wavelength λ. The inversion of equation (14) to solve for the size distribution $N(r)$, even assuming the complex index of refraction is known, is a very difficult task (Twomey and Howell, 1967). In this paper, we will not attempt to do this inversion. Instead, we will assume that a two-parameter model will be sufficient for the description of aerosol wavelength dependent extinction coefficient. We assume the two-parameter model to be of the following form

$$\beta_{aerosol}(\lambda) = A\, \lambda^{\alpha} \tag{15}$$

where A and α are the two parameters. The functional form of the aerosol extinction coefficient as expressed by equation (15) is identical to the result obtained by assuming the aerosols to have a Junge size distribution (Junge, 1963). Substituting equation (15) into (13), we then have a system of nonlinear equations with unknown $\beta_{mol}(\lambda_o)$, $\beta_{o3}(\lambda_o)$, A, and α for each altitude level. The system of nonlinear equations can be solved using the Marquardt (1963) algorithm. The Marquardt algorithm is a minimum search procedure for a system of nonlinear equations. An initial set of guessed solutions for the unknowns is updated through the following iterative equation

$$X^{(k+1)} = X^{(k)} - [J^T(x^k)\, J(x^k) + \lambda_k I]^{-1}\, J^T(x^k)\, F(x^k) \qquad (16)$$

where X^k is the solution vector for the unknowns at the k-iteration, $F(x^k)$ is the residue vector for equation (13) at the k-iteration, and $J(x^k)$ is the Jacobian matrix with element $J_{ij} = \partial f_i/\partial x_j$ where f_i is the ith nonlinear equation. I is the identity matrix, and λ_k is a control parameter at the k-iteration. The control parameter λ_k is adjusted at each iteration for fast convergence to the minimum. The iterative process is terminated when the difference between two consecutive residue squares is less than 0.1 percent.

INVERSION RESULTS

Inversion results have been obtained by applying the inversion techniques discussed above to simulated spacecraft solar extinction measurements. Several models of the aerosol and ozone profiles were used to generate atmospheric transmittance profiles at different wavelength regions. Wavelengths at 0.38, 0.45, 0.6, and 1.0 micron were chosen to coincide with the four spectral channel locations for the Stratospheric Aerosol and Gas Experiment (SAGE). The simulated radiant intensity data are generated from the atmospheric transmittance profiles by incorporating the spacecraft geometry. The radiometer is assumed to have a field of view of 30 arc seconds situated on a satellite at orbital altitude of 600 km. A total of 80 radiant intensity data points are generated per channel, covering tangent altitudes from 10 to 50 km in equal increments of half km height. Each data point is simulated by

assuming the radiometer is pointing to a different location on the solar disk.

The inversion of these radiant profiles was then performed by introducing experimental errors of various origin and magnitudes to the simulated data. There are three types of errors which directly affect the inversion results. The first type of error is the bias error in the determination of the exact tangent heights for all the data points. The second type of error is the noise associated with each measurement. The third type of error is associated with the uncertainty in knowing the pointing angle of the radiometer for each data point. This pointing error will result in both an erroneous value for the unattenuated solar radiants due to solar limb darkening effect and an erroneous value for the instantaneous tangent height.

The three types of errors mentioned above in different magnitudes were added to the simulated radiant data, and inversions were performed to determine the sensitivity of these errors on the inversion results. The atmosphere is divided into 45 homogeneous layers of half km thickness between 10 and 21 km, and increasing thickness from 21 to 50 km. The path length matrix is computed using a ray trace calculation to include atmospheric refraction effect.

Figures 3 to 6 show inversion results for simulated extinction measurements using the linear constrained inversion method. The input aerosol vertical profile used is deduced from an actual lidar backscattered profile with vertical resolution of 0.15 km. The ozone vertical profile used is similar to Elterman's model (1968) except that artificial layers structures were added. The Rayleigh extinction profile is also deduced from an actual rawinsonde temperature and pressure profile. In these simulated measurements experimental errors including noise level of 0.1 percent to full scale radiant intensity and pointing uncertainty of 3 arc seconds were added to the simulated measurements. The inversion results are presented in terms of aerosol vertical extinction at 1.0 micron (figure 3), ozone vertical extinction at 0.6 micron (figure 4), Rayleigh vertical extinction at 0.38 micron (figure 5), and aerosol optical model parameters (figure 6). The aerosol optical model parameter α is assumed to be -0.8 between 17 and 20 km and equal to -1.6 for the rest of the altitude range. Inspection of

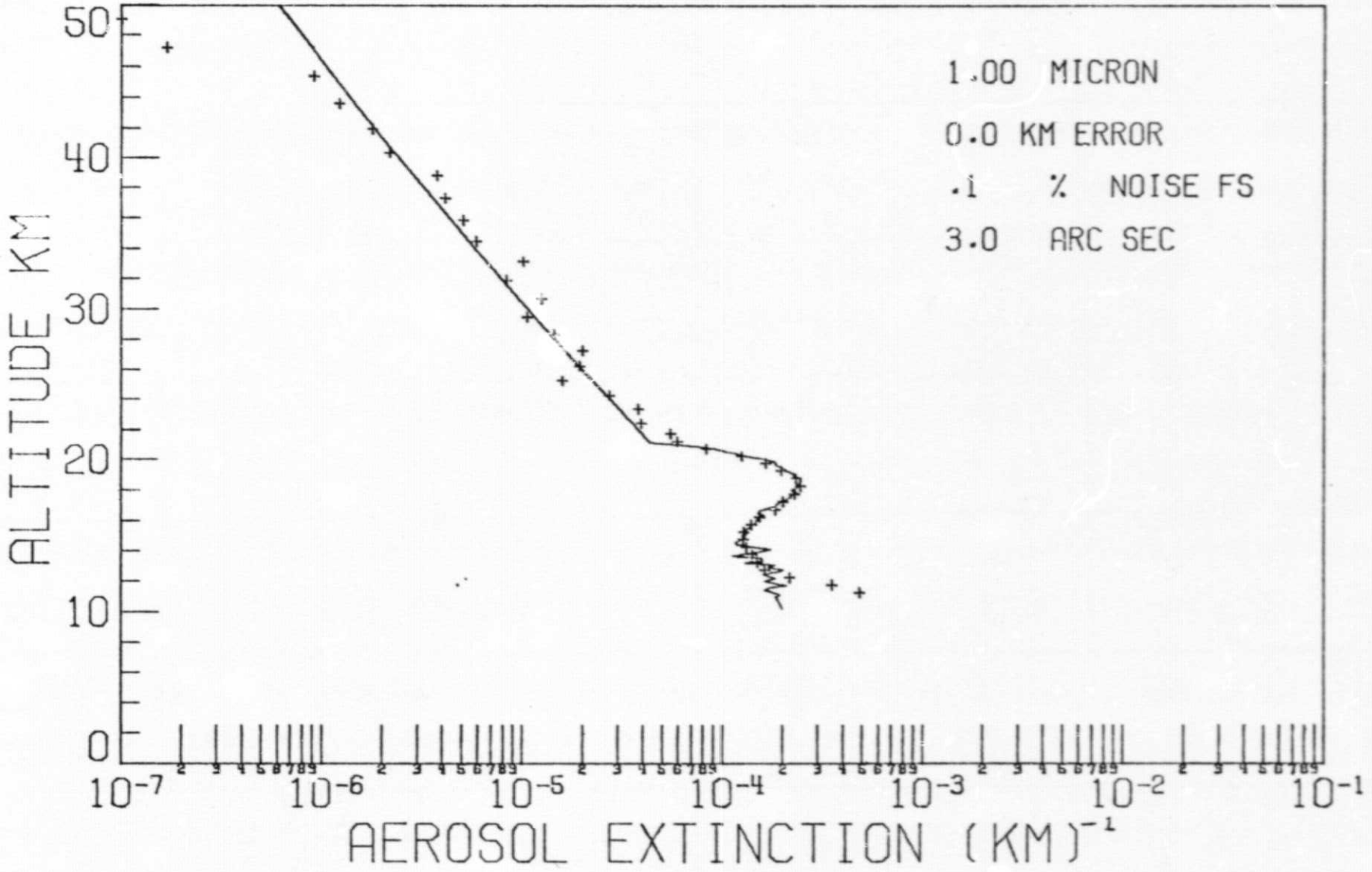

Figure 3. Inversion results for aerosol vertical extinction profile at 1.00 micron.

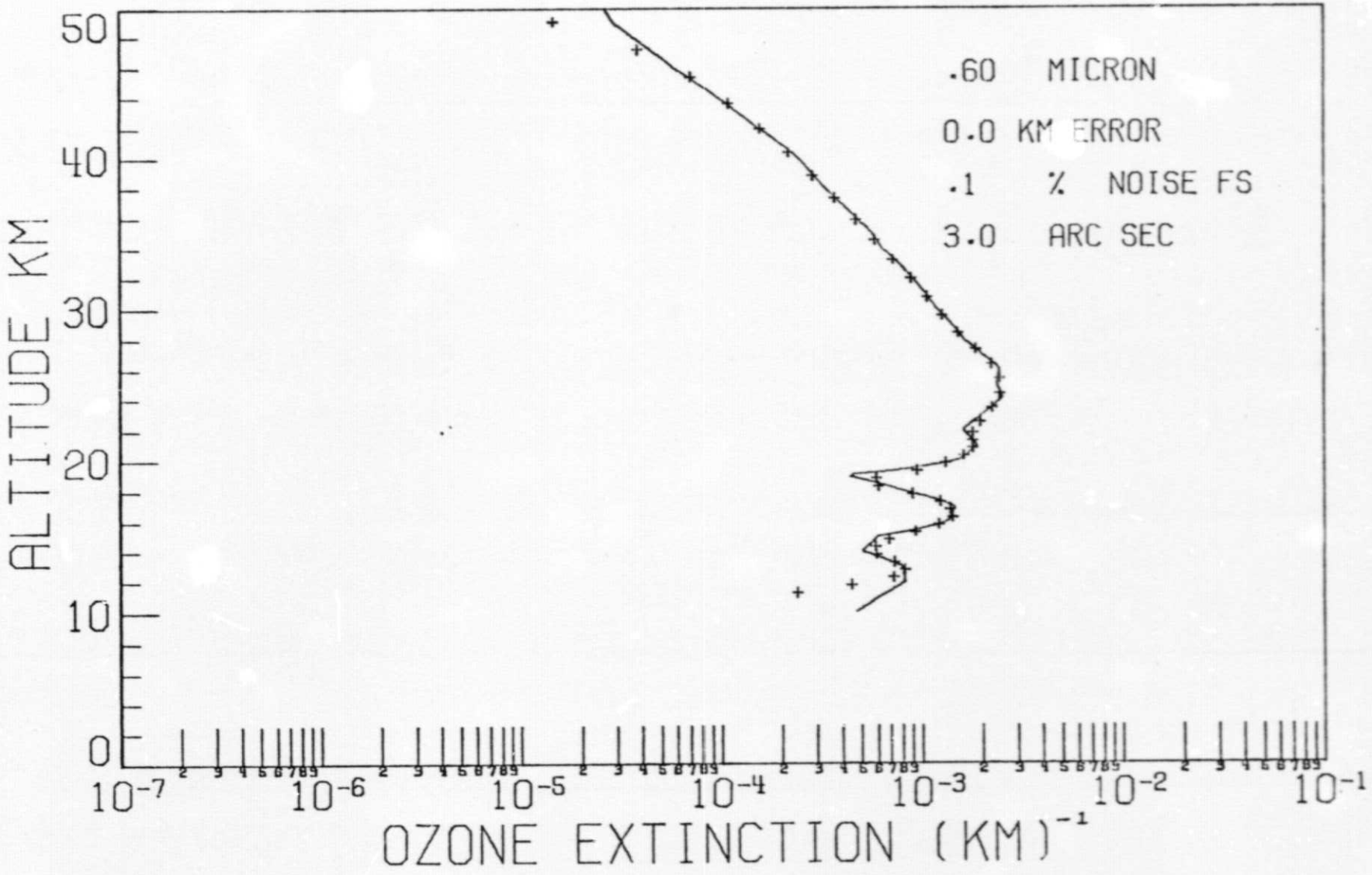

Figure 4. Inversion results for ozone vertical extinction profile at 0.6 micron.

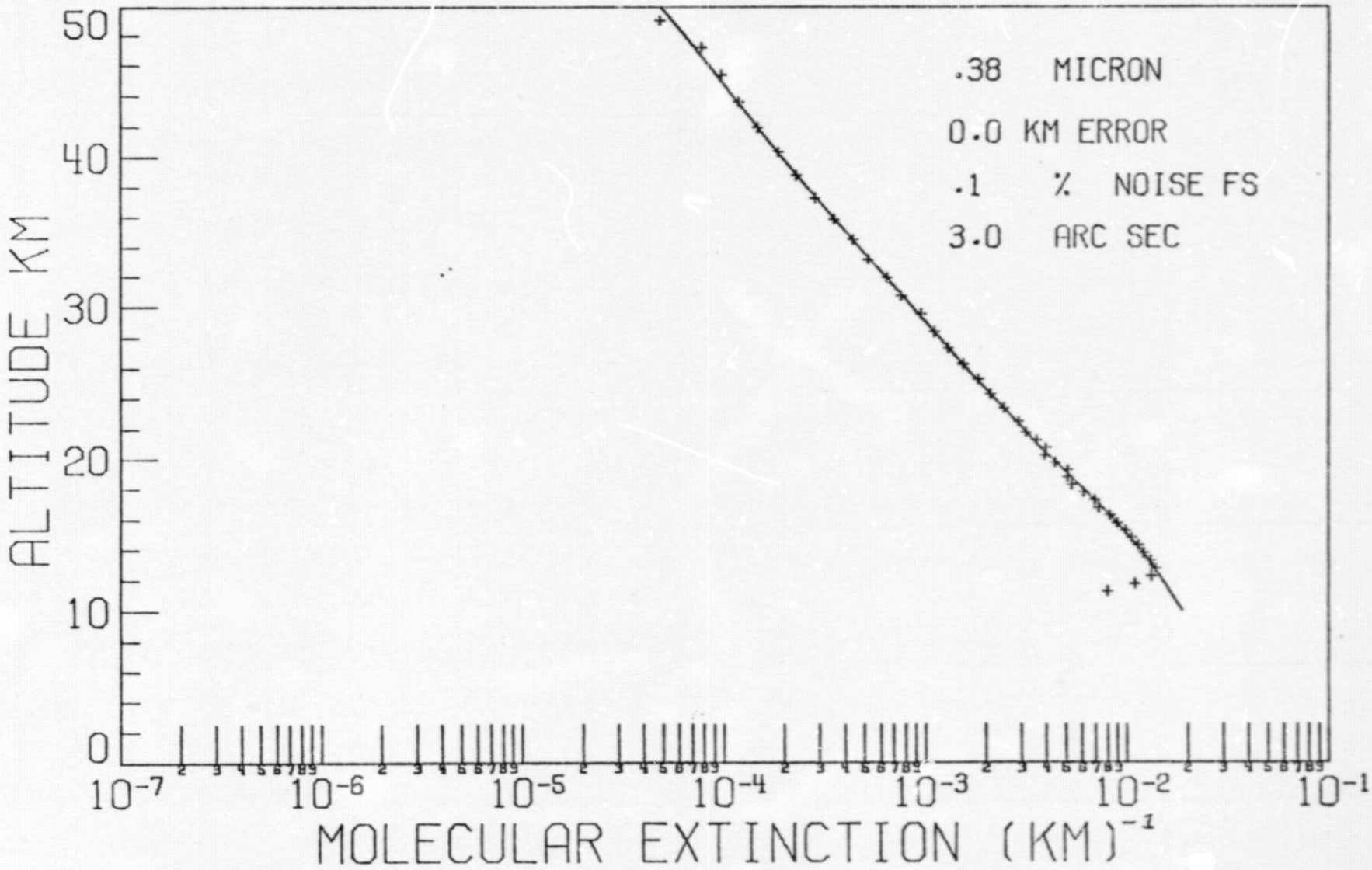

Figure 5. Inversion results for Rayleigh vertical extinction profile at 0.38 micron.

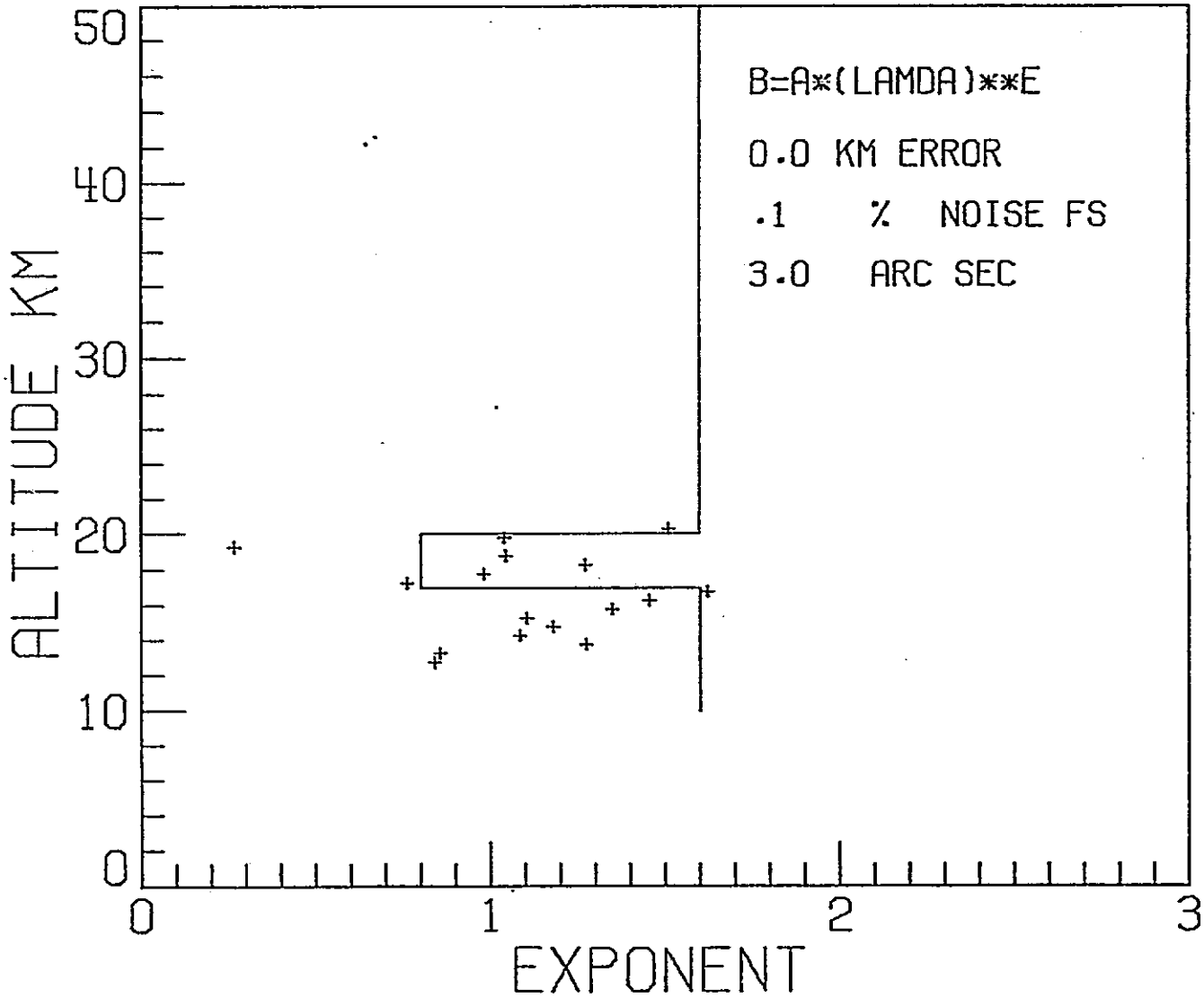

Figure 6. Inversion results for aerosol optical model parameter α as a function of altitudes.

figures 3 through 6 indicates that both aerosol and ozone vertical profiles can be inverted with good accuracy up to 40 km altitude. The poor inversion results for the Rayleigh profile below 14 km are caused by the rapidly decreasing signal level at the 0.38 micron channel. In figure 6, the inverted results for the aerosol optical parameter α within the Junge layer region show some fluctuation, and no inversion results can be obtained above 20 km due to the rapid decrease of aerosol concentration in this region.

Figures 7 to 9 show inversion results for the same input models except that the noise level for each measurement has been increased to 1.0 percent, and the pointing uncertainty has been increased to 15 arc seconds. Both the inverted results for aerosol and ozone profiles show considerable decrease in resolution. This behavior is consistent with the inversion technique in which the smoothing parameter α_0 in equation (11) is increased to accommodate the high noise level in the measurements. The inversion results for the aerosol optical model parameter which is not shown here are similar to figure 6 except larger fluctuations were observed.

Figures 10 and 11 show inversion results for different input aerosol and ozone vertical profiles. The aerosol profile is deduced from the first published lidar observation of the Volcano de Fuego eruption (McCormick et al., 1975) showing sharp layering structures. The peak layer at 19 km is approximately 0.5 km wide. The inversion cannot reproduce this sharp layering structure due to the integrating effect over the radiometer's field of view.

Figures 12 and 13 show the inversion results using the iterative method as discussed in equation (12). The atmospheric model and experimental noise levels are identical to those shown in figures 3 to 6. Comparison of the inversion results in this case to those shown in figures 3 and 4 indicates that they are quite similar. The inverted aerosol profile at altitudes above 30 km in this case shows some large amplitude oscillations. This is expected as the noise level in this altitude region is considerably higher than the signal level.

Inversions have also been performed on simulated data including bias errors in the tangent height determination. It is found that bias errors will produce a shift in altitude scale of the inverted profile in direct proportion to the bias magnitude.

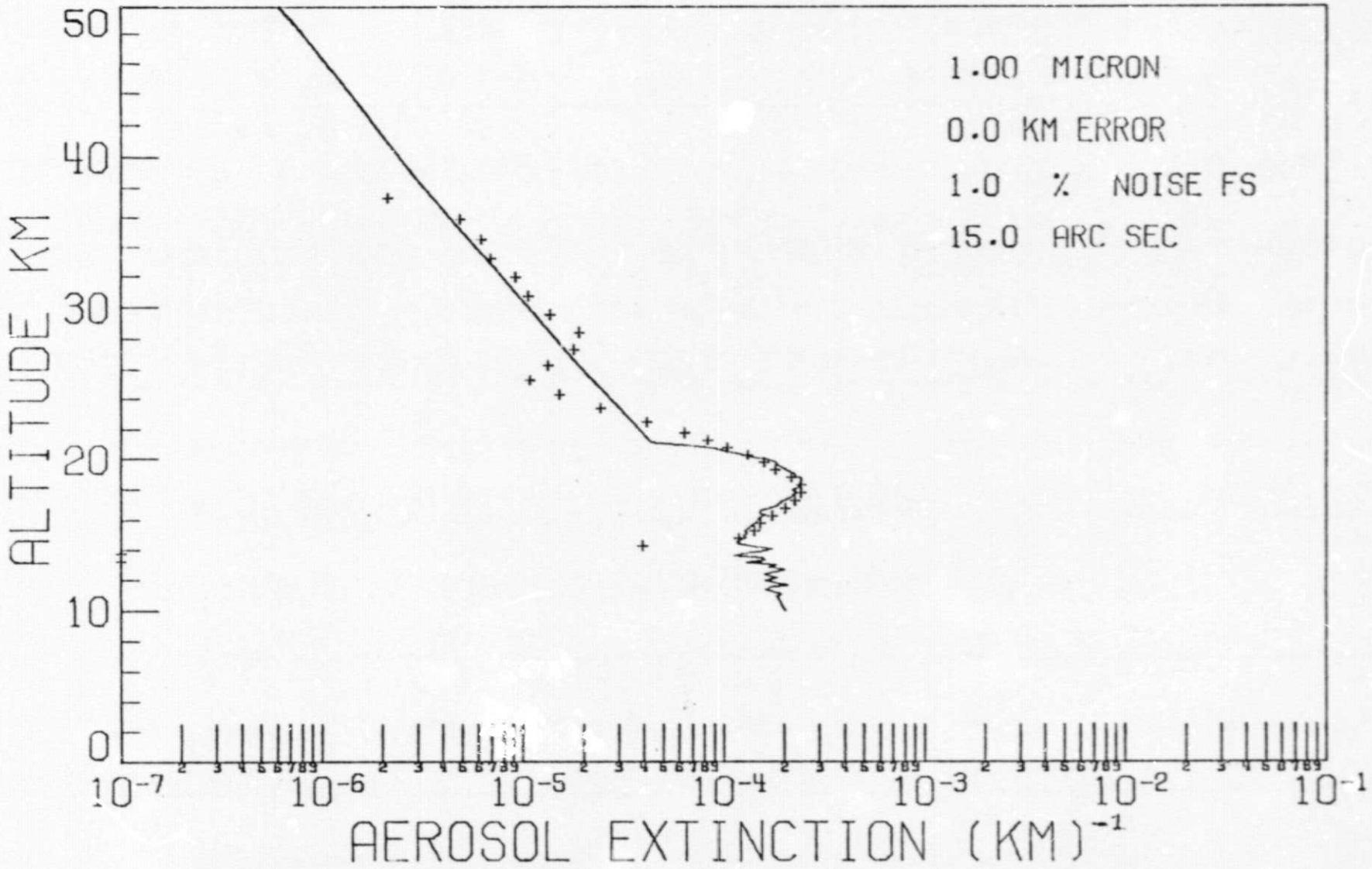

Figure 7. Same as figure 3 with increased experimental errors.

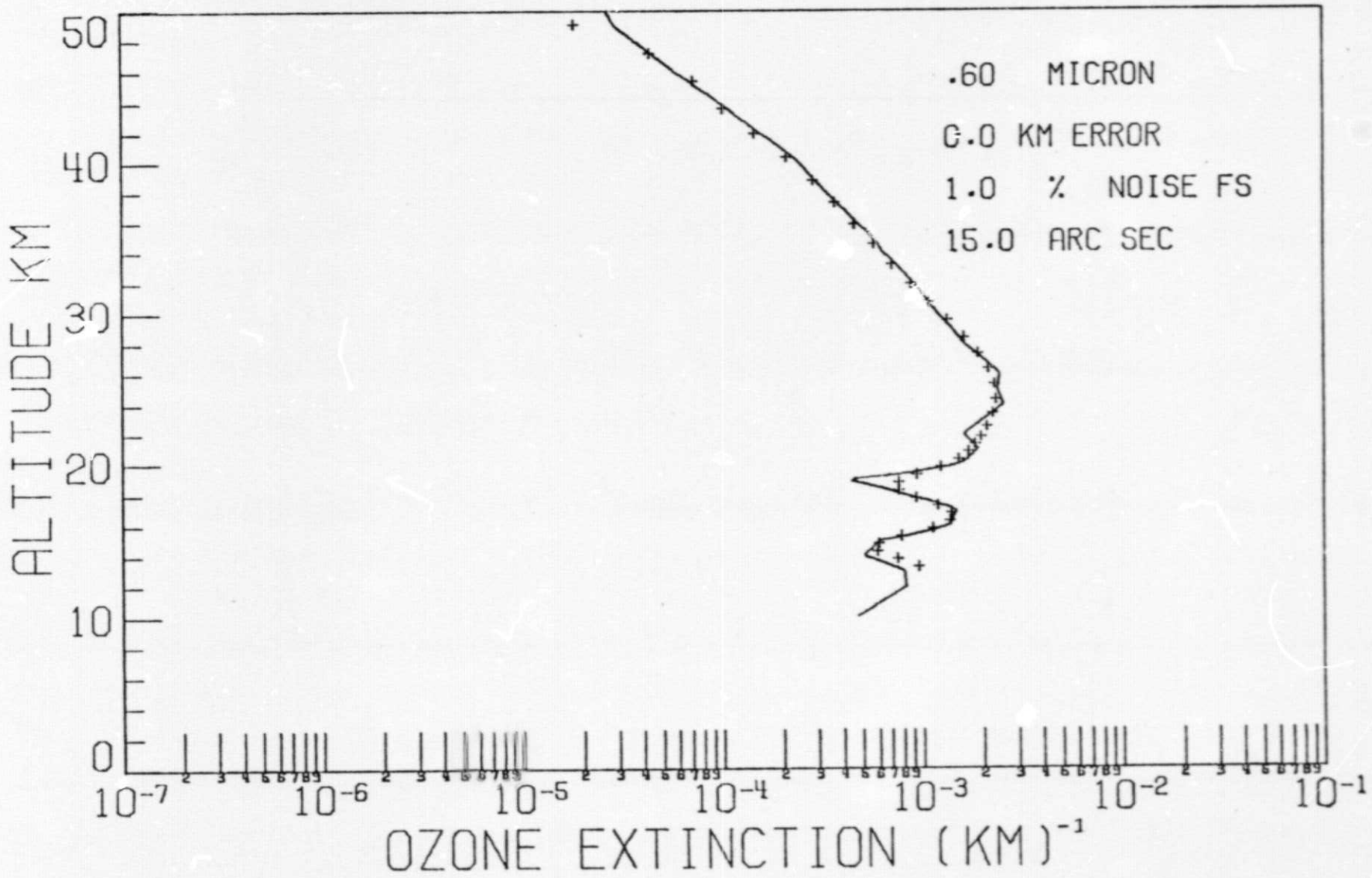

Figure 8. Same as figure 4 with increased experimental errors.

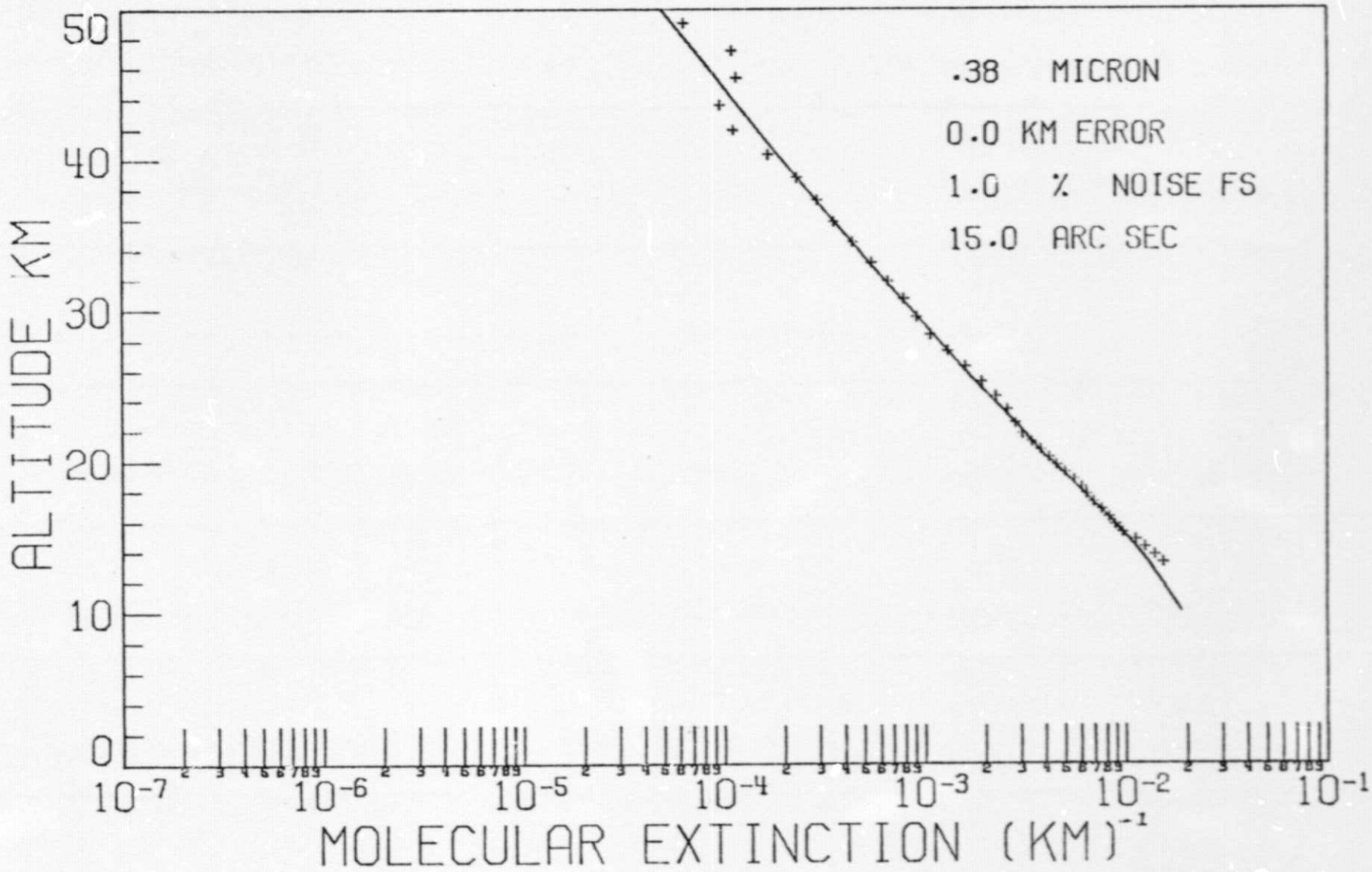

Figure 9. Same as figure 5 with increased experimental errors.

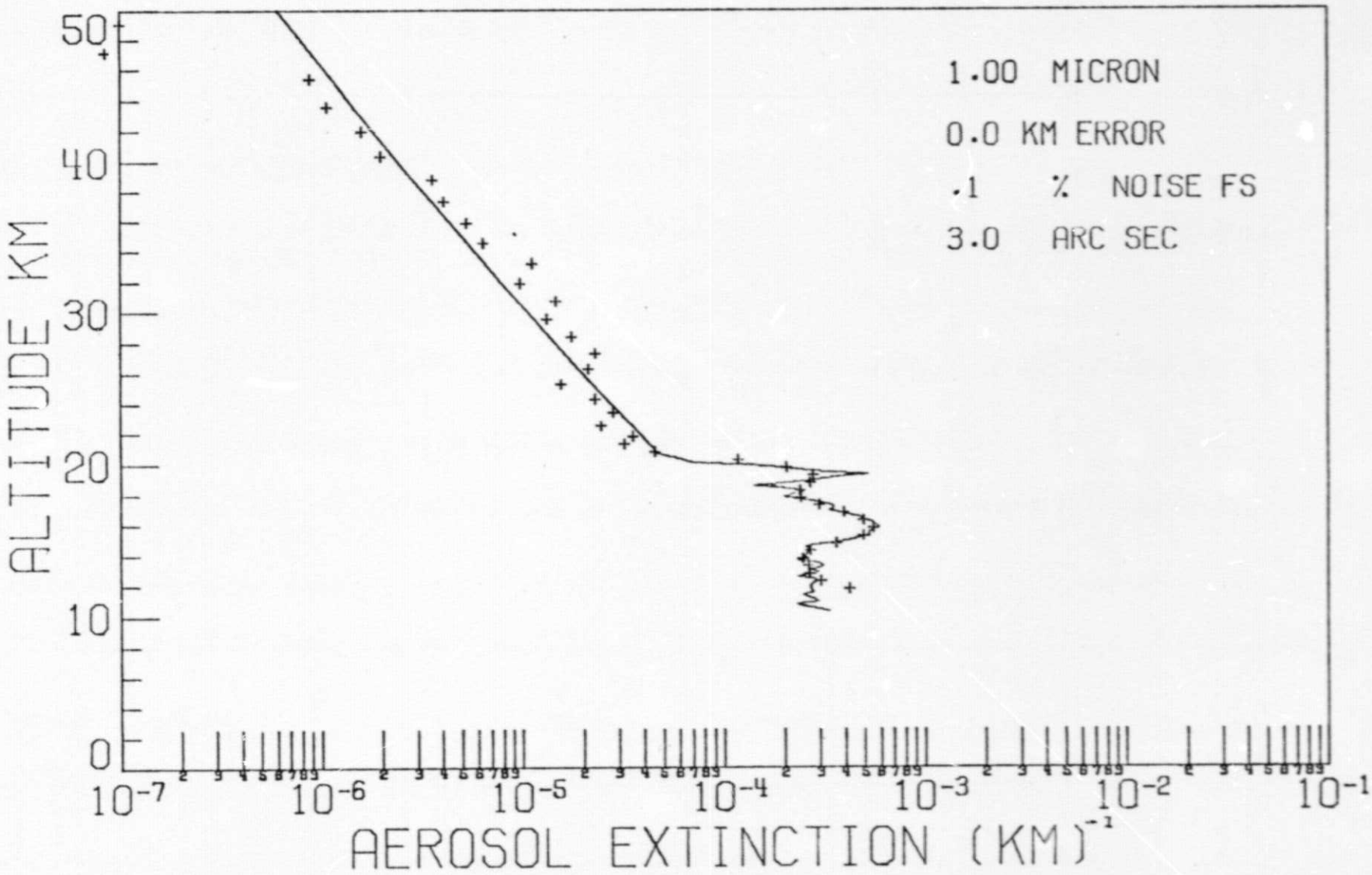

Figure 10. Same as figure 3 with different aerosol vertical extinction profile.

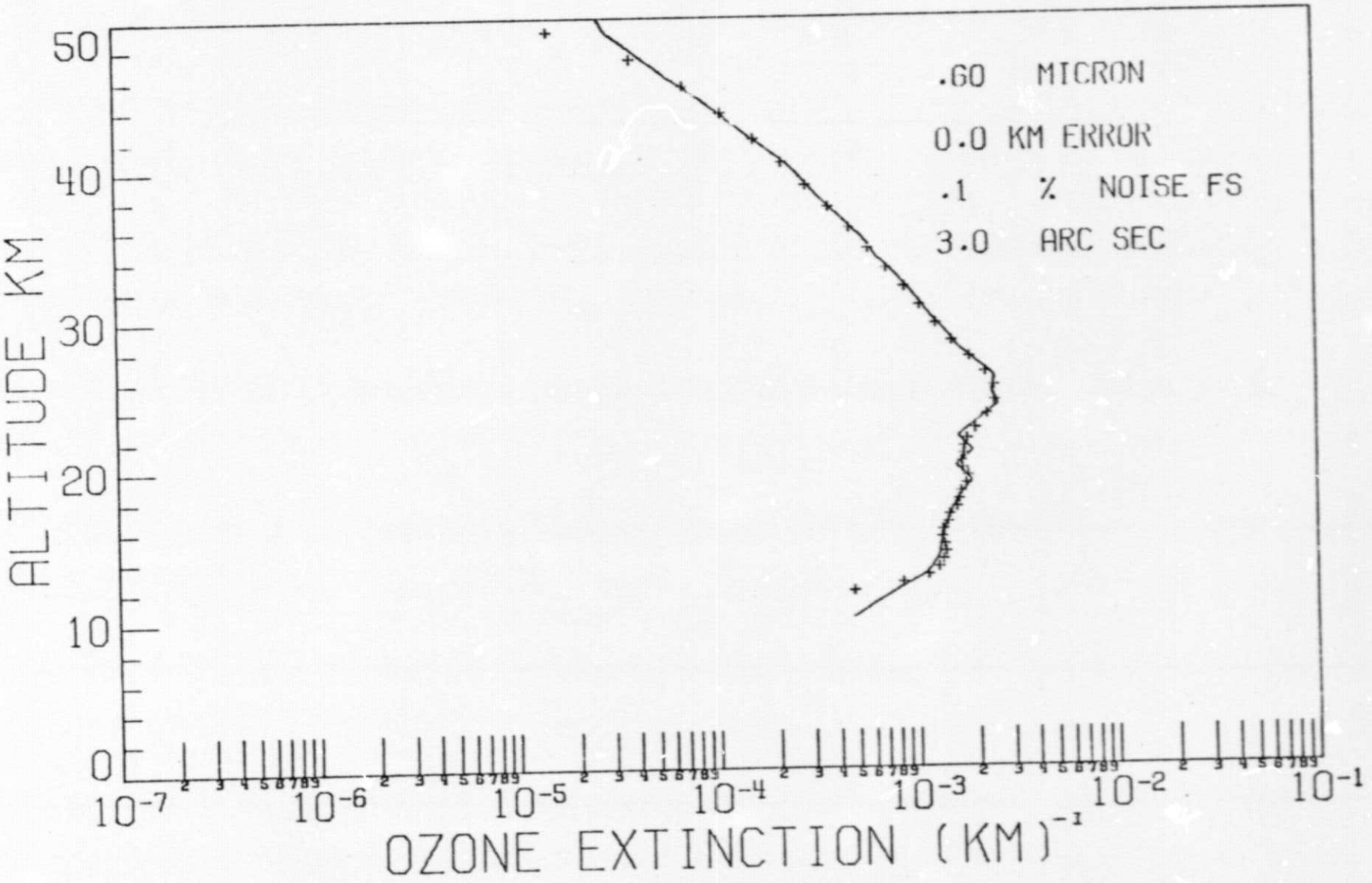

Figure 11. Same as figure 4 with different ozone vertical extinction profile.

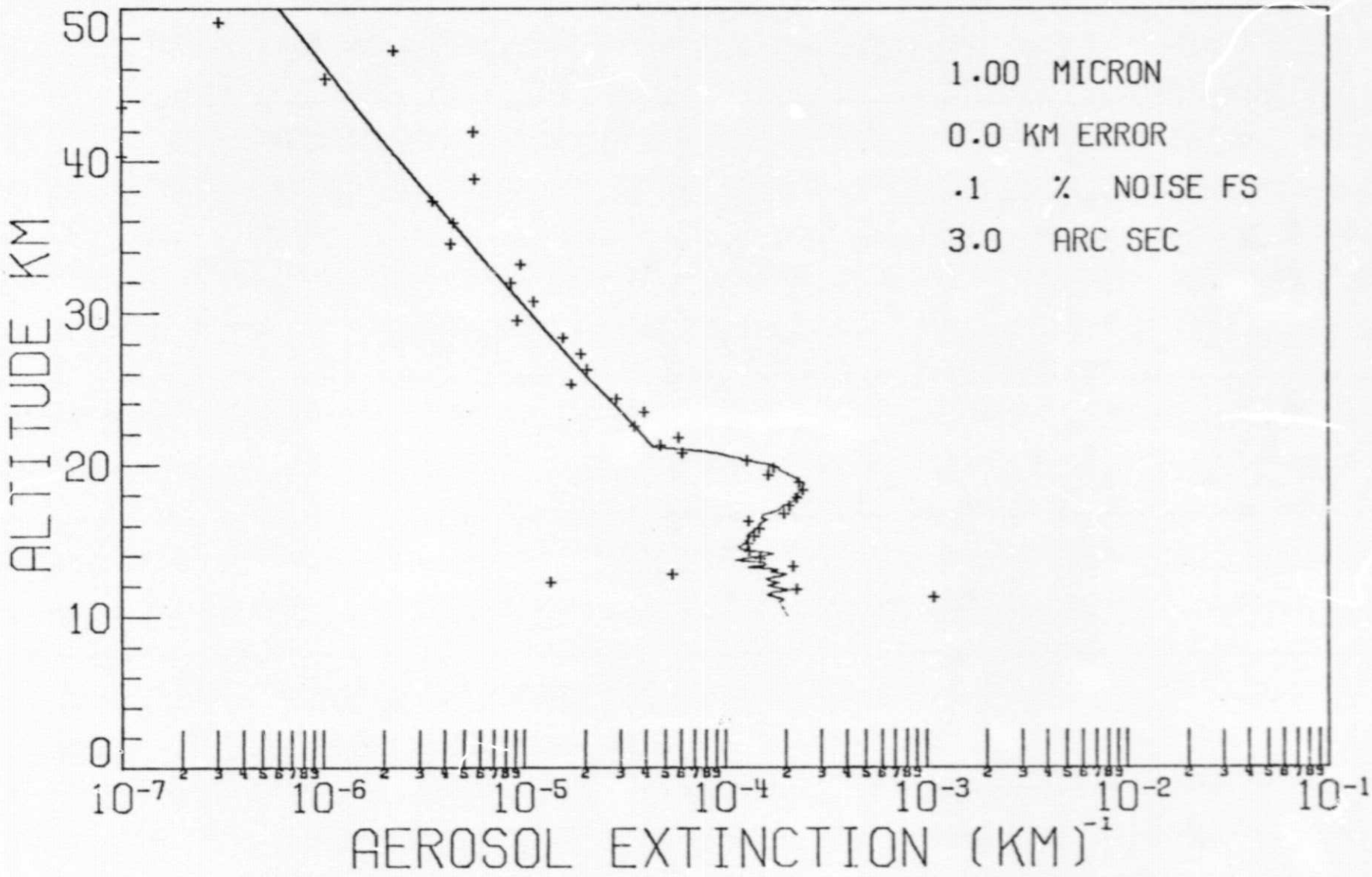

Figure 12. Same as figure 3 using the iterative inversion scheme.

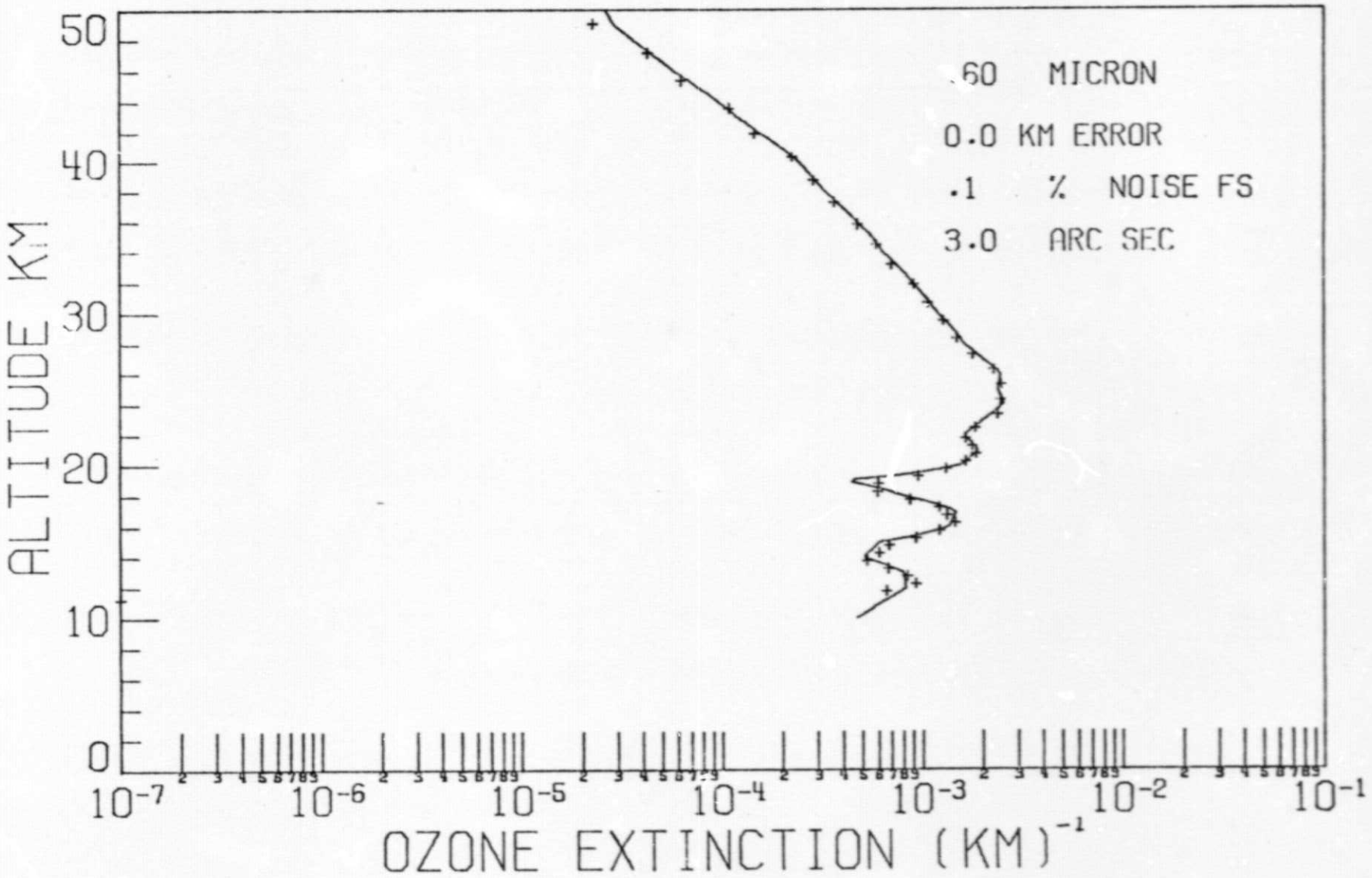

Figure 13. Same as figure 4 using the iterative inversion scheme.

CONCLUSIONS

This report has demonstrated that measurements from a spacecraft solar extinction experiment can be inverted to produce aerosol and ozone vertical profiles from cloud top up to approximately 50 km altitude. Analysis of the inversion results from simulated measurements including various experimental errors indicated that the resolution of the inverted profiles will be degraded as the errors are increased.

Both the linear constrained inversion method and the iterative method have been used for the inversion of solar extinction measurements. The accuracy of the inverted results from the two different inversion methods are similar.

REFERENCES

Chandrasekhar, S., "Radiative Transfer," Oxford University Press, 1950, p. 9.

Elterman, L., "Visible and IR Attenuation for Altitudes to 50 km," AFCRL-68-0153, Air Force Cambridge Research Laboratory, 1968.

Inn, E. C. Y., and Tanaka, Y., "Adsorption Coefficients of Ozone in the Ultraviolet and Visible Regions," J. Opt. Soc. Am., Vol. 43, p. 870, 1953.

Junge, C. E., "Air Chemistry and Radioactivity," Academic Press, New York, 1963, p. 142.

Marquardt, D. W., "An Algorithm for Least-Square Estimation of Nonlinear Parameters," J. Soc. Ind. Appl. Math., Vol. 11, p. 431, 1963.

McCormick, M. P., and Fuller, W. H., "Lidar Measurements of Two Intense Stratospheric Dust Layers," Applied Optics, Vol. 14, p. 4, 1975.

Phillips, D. L., "A technique for the Numerical Solution of Certain Integral Equations of the First Kind," J. Assn. Computing Machinery, Vol. 9, p. 97, 1962.

Twomey, S., "On the Numerical Solution of Fredholm Integral Equations of the First Kind by the Inversion of the Linear System Produced by Quadrature," J. Assn. Computing Machinery, Vol. 10, p. 99, 1963.

Twomey, S., and Howell, H. B., "Some Aspects of the Optical Estimations of Microstructure in Fog and Cloud," Applied Optics, Vol. 6, p. 2125, 1967.

Twomey, S., "Comparison of Constrained Linear Inversion and an Iterative Nonlinear Algorithm Applied to the Indirect Estimation of Particle Size Distributions," J. of Computational Physics Vol. 18, p. 188, 1975.